

3-D GRMHD Simulations of Generating Jets

K.-I. Nishikawa¹, S. Koide², K. Shibata³, T. Kudoh^{4,5}, H. Sol⁶

¹ National Space Science and Technology Center, 320 Sparkman Drive, SD 50, Huntsville, AL 35805, USA.

² Toyama University, Faculty of Engineering, 3190 Gofuku, Toyama 930-8555, Japan.

³ Kyoto University, Kwasan Observatory, Yamashina, Kyoto 607-8471, Japan.

⁴ National Astronomical Observatory, Mitaka, Tokyo 181-8588, Japan.

⁵ Department of Physics and Astronomy, University of Western Ontario London, Ontario N6A 3K7, Canada.

⁶ LUTH, Observatoire de Paris-Meudon, 92195 Meudon Cedex, France.

And

J. P. Hughes⁷, G. Richardson¹, R. Preece¹, P. Hardee⁸

⁷ Department of Physics and Astronomy, Rutgers, The State University of New Jersey, Piscataway, NJ 08854-8019, USA.

⁸ Department of Physics and Astronomy, The University of Alabama, Gallalee Hall, Tuscaloosa, AL 35487, USA.

Abstract. We have performed a first fully 3-D GRMHD simulation with Schwarzschild black hole with a free falling corona. The initial simulation results show that a jet is created as in the previous simulations using the axisymmetric geometry with the mirror symmetry at the equator. However, the time to generate the jet is longer than in the 2-D axisymmetric simulations. We expect that due to the additional freedom in the azimuthal dimension without axisymmetry with respect to the z axis and reflection symmetry with respect to the equatorial plane, the dynamics of jet formation can be modified. Further simulations are required for the study of instabilities along the azimuthal direction such as accretion-eject instability

1. Introduction

Relativistic jets have been observed in active galactic nuclei (AGNs) and micro-quasars in our Galaxy, and it is believed that they originate from the regions near accreting black holes or neutron stars [Meier, Koide, & Uchida]. To investigate the dynamics of accretion disks and the associated jet formation, we use a full 3-D GRMHD code. One of the most promising models for jet formation is the magnetic-acceleration model [Blandford & Payne]. The magnetic-acceleration mechanism has been proposed not only for AGN jets, but also for protostellar jets (see [Meier, Koide, & Uchida]).

Recently, Koide, Shibata, & Kudoh (1999) [Koide, Shibata, & Kudoh] have investigated the dynamics of an accretion disk initially threaded by a uniform poloidal magnetic field in a non-rotating corona (either in a state of steady fall or in hydrostatic equilibrium) around a non-rotating black hole. The numerical results show that the disk loses angular momentum by magnetic braking, then falls into the black hole. The infalling motion of the disk, which is faster than

in the non-relativistic case because of the general-relativistic effect below $3r_S$ (r_S is the Schwarzschild radius), is strongly decelerated at the shock formed by the centrifugal force around $r = 2r_S$ by the rotation of the disk. Plasmas near the shock are accelerated by the $\mathbf{J} \times \mathbf{B}$ force, which forms bipolar relativistic jets. Inside this *magnetically driven jet*, the gradient of gas pressure also generates a jet over the shock region (*gas-pressure-driven jet*). This *two-layered jet structure* is formed both in a hydrostatic corona and in a steady-state falling corona. Koide et al. (2000) [Koide et al 2000] have also developed a new GRMHD code in Kerr geometry and have found that, with a rapidly rotating ($a = 0.95$) black-hole magnetosphere, the maximum velocity of the jet is $0.9 c$ and its terminal velocity $0.85 c$. All of the previous 2-D GRMHD simulations described here were made assuming axisymmetry with respect to the z -axis and mirror symmetry with respect to the plane $z = 0$; the axisymmetric assumption suppressed the azimuthal instabilities.

2. 3-D GRMHD Simulations: Equations and Numerical Techniques

Our basic equations are those of Maxwell for the fields and a set of general-relativistic equations representing the plasma, namely the equations of conservation of mass, momentum, and energy for a single-component conducting fluid [Weinberg 1972, Thorne, Price, and Macdonald 1986, Koide, Shibata, & Kudoh].

Our simulations employ the equations of general-relativistic MHD together with the Simplified Total-Variation-Diminishing (STVD) method. The STVD method was developed by Davis (1984) [Davis 1984] for studying violent phenomena such as shocks [Nishikawa *et al.* 1997, Koide, Shibata, & Kudoh]. This method is as Lax-Wendoroff's method with additional diffusion term. We have checked that this method respects the energy-conservation law and its propagation properties [Koide, Shibata, & Kudoh].

3. Initial 3-D GRMHD simulations with a Schwarzschild black hole

In order to investigate how accretion disks near black holes evolve under the influence of accretion instabilities such as the magnetorotational instability [Balbus & Hawley 1998] and accretion-ejection instability (AEI) [Tagger & Pellat, 1999], the use of a fully 3-D GRMHD is essential.

3.1. Initial and boundary conditions

In the assumed initial state, the simulation region is divided into two parts: a background corona around a black hole, and an accretion disk (Fig. 1a). The coronal plasma is set in a state of transonic free-fall flow, as in the case of the transonic flows with $\Gamma = 5/3$ and $H = 1.3$; here the sonic point is located at $r = 1.6r_S$. The Keplerian disk in the corona is set in the following way. The disk region is located at $r > r_D \equiv 3r_S, |\cos\theta| < \delta = 1/8$. Here the density is 100 times that of the background corona (Fig. 1a), while the orbital velocity is relativistic and purely azimuthal: $v_\phi = v_K \equiv c/[2(r/r_S - 1)]^{1/2}$. (Note that this equation reduces to the Newtonian Keplerian velocity $v_\phi = \sqrt{GM/r}$ in the non-relativistic limit $r_S/r \ll 1$). The pressure of both the corona and the disk are assumed equal to that of the transonic solution. The initial conditions for the entire plasma around the black hole are: $\rho = \rho_{\text{ffc}} + \rho_{\text{dis}}$

$$\rho_{\text{dis}} = \begin{cases} 100\rho_{\text{ffc}} & (r > r_{\text{D}} \text{ and } |\cot\theta| < \delta) \\ 0 & (r \leq r_{\text{D}} \text{ or } |\cot\theta| \geq \delta) \end{cases} \quad (1)$$

$$(v_r, v_\theta, v_\phi) = \begin{cases} (0, 0, v_{\text{K}}) & (r > r_{\text{D}} \text{ and } |\cot\theta| < \delta) \\ (-v_{\text{ffc}}, 0, 0) & (r \leq r_{\text{D}} \text{ or } |\cot\theta| \geq \delta) \end{cases} \quad (2)$$

where we set $\delta = 0.125$; the smoothing length is $0.3r_{\text{S}}$.

In addition, there is a magnetic field crossing the accretion disk perpendicularly. We set it to the Wald solution [Wald 1974], which represents the uniform magnetic field around a Kerr black hole: $B_r = B_0 \cos\theta$, $B_\theta = -\alpha B_0 \sin\theta$ (where α is the lapse function, $\alpha = (1 - r_{\text{S}}/r)^{1/2}$). At the inner edge of the accretion disk, the proper Alfvén velocity is $v_{\text{A}} = 0.015c$ in a typical case with $B_0 = 0.3\sqrt{\rho_0 c^2}$, where the Alfvén velocity in the fiducial observer, $v_{\text{A}} \equiv B/\sqrt{\rho + [\Gamma p/(\Gamma - 1) + B^2]/c^2}$. The plasma beta of the corona at $r = 3r_{\text{S}}$ is $\beta \equiv p/B^2 = 1.40$. The simulation is performed in the region $1.1r_{\text{S}} \leq r \leq 20r_{\text{S}}$, $0 \leq \theta \leq \pi$, $0 \leq \phi \leq 2\pi$ with $100 \times 120 \times 60$ meshes. The effective linear mesh widths at $r = 1.1r_{\text{S}}$ and at $r = 20r_{\text{S}}$ are $5.38 \times 10^{-3}r_{\text{S}}$ and $0.97r_{\text{S}}$, respectively, while the angular spacings along the polar and azimuthal directions are 5.2×10^{-2} rad. A radiative boundary condition is imposed at $r = 1.1r_{\text{S}}$ and at $r = 20r_{\text{S}}$. The computations were made on an ORIGIN 2000 computer with 0.898 GB internal memory, and they used about 47 hours of CPU time for 10000 time steps with $100 \times 120 \times 60$ meshes.

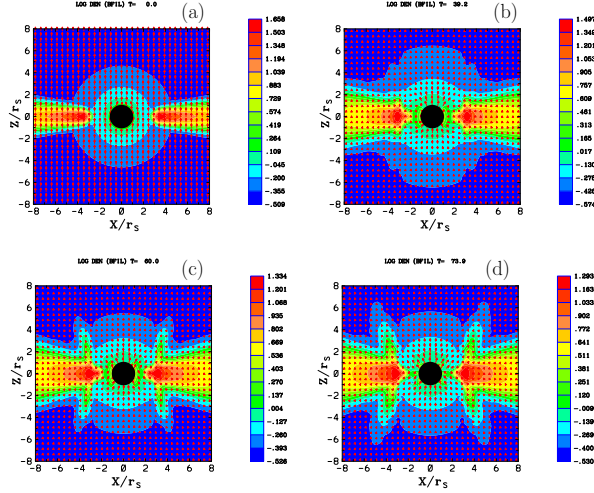


Figure 1. For the fully 3-D simulation, these panels present the time evolution of the proper mass density with the magnetic field (B_x, B_z) in a transonic free-fall (steady-state falling) corona with an initially uniform magnetic field, at $t = 0.0\tau_{\text{S}}$ (a), $t = 39.3\tau_{\text{S}}$ (b), $t = 60.0\tau_{\text{S}}$ (c), and $t = 73.9\tau_{\text{S}}$ (d). The jet is formed around $r = 4.5r_{\text{S}}$ as in the 2-D simulation.

3.2. Simulation results

Figure 1 shows the evolution of 3-D simulation performed in the region $1.1r_{\text{S}} \leq r \leq 20r_{\text{S}}$, $0 \leq \theta \leq \pi$, and $0 \leq \phi \leq 2\pi$ with $100 \times 120 \times 60$ meshes. The parameters used in this simulation are the same as those of the axisymmetric simulations

shown in Fig. 6 of [Koide, Shibata, & Kudoh]. In this figure, the colored shading shows the proper mass density on logarithmic scales; the vector plots show the magnetic field.

The black circle represents the black hole. Figures 1a presents the initial conditions, which are the same as in the 2-D simulations [Koide, Shibata, & Kudoh]. At $t = 39.2\tau_S$ (Fig. 1b) comparing with Fig. 6c ($t = 40.0\tau_S$) in [Koide, Shibata, & Kudoh] the jet is less generated. At $t = 60.0\tau_S$ as shown in Fig. 1c, the jet is generated as 2-D simulation at the earlier time ($t = 40.0\tau_S$). At $t = 73.9\tau_S$, the jet is clearly created around $r = 4.5r_S$, which is shown by the enhanced density (Fig. 1d). As in the 2-D simulations the jet is generated in a hollowed cylindrical form.

The delay of jet formation seems to be due to reduction of shock formation at $r = 2r_S$ caused by the additional freedom in the azimuthal direction. Further investigation will be reported elsewhere.

4. Discussion

Recently, review articles on magnetohydrodynamic production of relativistic jets have reported unsolved questions related to jet formation and its mechanisms which determine the velocity of jets and time variations of jet flux [Meier, Koide, & Uchida, Blandford 2001, Meier 2002].

This simulation result is initial and we will perform more simulations and investigate effects of the third dimension. This simulation study will be extended to understand the different (high/soft and low/hard) states [Fender(2001)] and different combination of accreting rate $\dot{m} \equiv \dot{M}/\dot{M}_{Edd}$ and the angular momentum $j \equiv J/J_{\max}$ [Meier 2002]. Further results will be reported elsewhere.

Acknowledgments

K.N. is partially supported by NSF ATM 9730230, ATM-9870072, ATM-0100997, and INT-9981508. The simulations have been performed on ORIGIN 2000 at NCSA which is supported by NSF.

References

- Meier, Koide, & Uchida.. Meier, Koide, & Uchida, 2001, *Science*, **291**, 84.
 Blandford & Payne.. Blandford & Payne, 1982, *MNRAS*, **199**, 883.
 Koide, Shibata, & Kudoh.. Koide, Shibata, & Kudoh, 1999, *ApJ*, **522**, 727.
 Koide et al 2000.. Koide, Meier, Shibata, & Kudoh, 2000, *ApJ*, **536**, 668.
 Weinberg 1972.. Weinberg, 1972, *Gravitation and Cosmology* (New York: Wiley)
 Thorne, Price, and Macdonald 1986.. Thorne, Price, and Macdonald, 1986, *Black Holes: The Membrane Paradigm* (New Haven: Yale Univ. Press)
 Davis 1984.. Davis, 1984 NASA Contractor Rep. 172373, ICASE Rep., No. 84-20.
 Nishikawa *et al.* 1997.. Nishikawa, Koide, Sakai, Christodoulou, Sol, & Mutel, 1997, *ApJ*, **483**, L45.
 Balbus & Hawley 1998.. Balbus, & Hawley, 1998, *RMP*, **70**, 1.
 Tagger & Pellat, 1999.. Tagger, & Pellat, 1999, *A&A*, **349**, 1003.

Wald 1974.. Wald, 1974, Phys. Rev. D., 10, 1680.

Blandford 2001.. Blandford, 2001, Prog. Theor. Phys. Suppl. **143**, 182.

Meier 2002.. Meier, D. 2002, NewAR, **46**, 247.

Fender(2001).. Fender, 2001, Relativistic flows in Astrophysics, in press, astro-ph/0109502.